ELSEVIER

Neurobiology of Aging xxx (2008) xxx–xxx

NEUROBIOLOGY OF AGING

www.elsevier.com/locate/neuaging

Potential amyloid plaque-specific peptides for the diagnosis of Alzheimer's disease

Lionel Larbanoix [a], Carmen Burtea [a], Sophie Laurent [a], Fred Van Leuven [b], Gérard Toubeau [c], Luce Vander Elst [a], Robert N. Muller [a,*]

[a] *Department of General, Organic and Biomedical Chemistry, NMR and Molecular Imaging Laboratory, University of Mons-Hainaut, 24 Avenue du Champ de Mars, B-7000 Mons, Belgium*

[b] *Experimental Genetics Group, KULeuven, Herestraat 49, B-3000 Leuven, Belgium*

[c] *Department of Histology, University of Mons-Hainaut, 6 Avenue du Champ de Mars, B-7000 Mons, Belgium*

Received 26 February 2008; received in revised form 23 June 2008; accepted 30 September 2008

Abstract

Amyloid plaques (AP) represent one of the main molecular hallmarks of Alzheimer's disease (AD). In order to develop new AP-specific contrast agents for AD molecular imaging, the phage display technology was used to identify peptides specific to amyloid-beta ($A\beta_{42}$).

A random disulfide constrained heptapeptide phage display library was screened against $A\beta_{42}$. After biopanning, 72 phage clones were isolated and their binding affinity to $A\beta_{42}$ was evaluated by enzyme-linked immunosorbent assay (ELISA). The final library was enriched in two peptide sequences. The K_d of candidate phage clones for binding to $A\beta_{42}$ are in the picomolar range. The binding affinity for $A\beta_{42}$ of two selected peptides was confirmed by ELISA, and the specific interaction with AP was validated by immunohistochemistry on brain sections. The preliminary MRI *in vivo* study, which was performed with a peptide functionalized contrast agent on AD transgenic mouse, showed encouraging results.

To conclude, low molecular weight peptides presenting a specific affinity for $A\beta_{42}$ were identified by phage display. As specific carriers, they have a real potential for molecular imaging of AD thanks to AP binding.

Keywords: Alzheimer's disease; Amyloid-beta; Molecular imaging; Phage display; Amyloid plaques

1. Introduction

The neurodegenerative disorder known as Alzheimer's disease (AD) is the fourth cause of mortality in the developed countries (after cancer, brain stroke, and cardiovascular pathologies) and the leading cause of dementia in the elderly. AD is responsible for the loss of cognitive abilities, such as memory, speech, and computing, the patients become confused and their behavior is radically changed. The autopsy of AD patients revealed cortical atrophy and the increased size of ventricles associated to the presence of neurofibrillary tangles (NFTs) and of beta-amyloid plaques (AP) that are the major pathologic hallmarks of AD. AP are essentially composed of amyloid-beta (Aβ) peptides, often do not surpass 200 μm in diameter, and are located in the interstitial spaces of the brain. Aβ, either associated in oligomers or aggregated in AP, can play a key neurotoxic role by disturbing the synaptic function, by creating the conditions of oxidative stress and of localized inflammation, as well as by inducing the formation of NFTs (Huang et al., 1999; Iversen et al., 1995; Rapoport and Ferreira, 2000; Rogers and Lue, 2001). Most Aβ peptides are composed of 40 ($A\beta_{40}$) or 42 ($A\beta_{42}$) amino acids and are produced by two successive proteolytic cleavages of the trans-membrane protein known as amyloid precursor protein (APP), consecutively by β-secretase and γ-secretase (Hartmann et al., 1997). $A\beta_{42}$ is the least soluble and thereby the major trigger of neuritic plaques, while amyloid deposition adjacent to blood vessels are enriched in $A\beta_{40}$ (Van Dorpe et al., 2000). By molecular interactions,

* Corresponding author. Tel.: +32 65 373520; fax: +32 65 373520.
E-mail address: robert.muller@umh.ac.be (R.N. Muller).

0197-4580/$ – see front matter © 2008 Elsevier Inc. All rights reserved.
doi:10.1016/j.neurobiolaging.2008.09.021

Aβ peptides form soluble protofibrils that then aggregate into insoluble fibrils and AP (Sipe, 2005).

Essentially based on cognitive tests, the diagnosis of AD becomes more definitive only at later stages of the disease, after the apparition of serious mental problems, i.e. when much of the brain is already severely damaged. Nevertheless, volumetric and functional approaches performed with magnetic resonance imaging (MRI) or positron emission tomography (PET) scanners provide complementary information that can exclude other pathologies and help AD diagnosis (Jagust et al., 2007). Unfortunately, these methods are not specific, and do not have enough spatial resolution (PET) or sensitivity (MRI) to identify small lesions.

The development of new molecular imaging techniques (Boutry et al., 2005; Burtea et al., 2008; Segers et al., 2007; Weissleder and Mahmood, 2001) offers novel perspectives for medical diagnosis by the detection of biochemical abnormalities of the diseases, whereas classical imaging techniques are only able to show the morphological consequences of these alterations. In this context, numerous efforts are devoted to develop new specific-targeted contrast agents, to amplify the signals, and to improve imaging techniques. In the case of AD diagnosis, imaging of AP appears to be the most convenient because they are characteristic to this pathology, they have a relatively large size, and are situated extracellularly. Current strategies are studied mostly by micro-PET or micro-MRI with the design of contrast agents that accumulate on AP areas thanks to specific ligands. For PET, derivatives of small aromatic compounds have been generally used, such as Congo Red or thioflavin-S that bind to beta-sheet structures. The best studied compounds for AP detection in human brain are *N*-methyl-11C-2-(4′-methylaminophenyl)-6-hydroxy-benzothiazole (Pittsburgh Compound-B or PIB) and 2-(1-[6-{(2-[F-18]fluoroethyl)(methyl)amino}-2-naphthyl]ethylidene)malononitrile (FDDNP) (Nordberg, 2008). For MRI, the contrast agents have been frequently functionalized with $A\beta_{40}$-derived peptides, but Congo Red derivatives have also been utilized (Higuchi et al., 2005; Poduslo et al., 2004; Sigurdsson et al., 2007; Wadghiri et al., 2003). It seems that the iron and calcium content of AP allows their detection with specific MRI acquisition sequences without any contrast agent (Benveniste et al., 1999; Borthakur et al., 2006; Brass et al., 2006; Dhenain et al., 2007; Jack et al., 2004; Lee et al., 2004; Vanhoutte et al., 2005). Unfortunately, it requires very high magnetic fields (7 T or more) and very long acquisition times (i.e. several hours) that are not practicable in clinical MRI. Moreover, the pre-clinical detection of endogenous iron is also dependent on the plaques' nature (i.e. not all plaques contain iron), as well as on the stage of the disease (i.e. larger plaques may contain more iron, increasing their detectability).

The development of small and natural pharmacological compounds represents a new research field of clinical interest. Among them, peptides are particularly interesting for the functionalization of contrast agents. As compared to larger molecules such as proteins, the advantages of peptides are their lower immunogeneicity and cost of synthesis, easier diffusion towards targeted sites, as well as their greater *in vivo* stability.

Phage display technology is one of the most frequently used screening tools for the identification of peptide ligands able to target any type of biomolecules (Smith and Petrenko, 1997; Zwick et al., 1998). This technique consists in the insertion of a foreign DNA fragment (oligonucleotide) in the structural gene of bacteriophages, which leads to the expression of a peptide at the surface of the viral particle. Random distribution of codons in the insert results in the construction of a peptide library often containing one billion of different peptides. Recently, 20-mer and 12-mer peptides were screened against Aβ (Kang et al., 2003; Orner et al., 2006; Wiesehan et al., 2003). Although with a specific affinity for Aβ, the large size of these peptides represents an important drawback for the vectorization of specific contrast agents towards the targeted molecular structures.

In the present work, we have performed the biopanning of a disulfide constrained heptapeptide phage display library to identify ligands with specific affinities for $A\beta_{42}$. In addition to other advantages cited above, the constraints imposed on peptides by disulfide bridges may confer spatial conformations that possess a far higher binding activity than any unconstrained peptide (Smith and Petrenko, 1997). We have evaluated the binding affinities of different selected clones for $A\beta_{42}$. Two derived peptides were chosen, synthesized, and investigated by enzyme-linked immunosorbent assay (ELISA) and by immunohistochemistry on the brain of a mouse model of AD. Finally, a preliminary *in vivo* MRI study, in addition to a pharmacokinetics and biodistribution evaluation, was performed with a peptide functionalized contrast agent on a transgenic mouse model of AD.

2. Materials and methods

2.1. Biopanning of PhD-C7C phage display library against $A\beta_{42}$

A random disulfide constrained heptapeptide library (PhD-C7C, New England Biolabs Inc., Leusden, The Netherlands) was used for biopanning against the mouse $A\beta_{42}$ (Bachem AG, Bubendorf, Switzerland). The well of an ELISA plate (Greiner Bio-One, Wemmel, Belgium) was coated with 150 μl of $A\beta_{42}$ (22.6 μM in 0.1 M $NaHCO_3$ buffer, pH 8.6) overnight at 4 °C. The next day, the solution was discarded and the well was blocked for 2 h at 4 °C with 200 μl of blocking buffer (0.1 M $NaHCO_3$, pH 8.6, 0.02% NaN_3, 0.5% bovine serum albumin (BSA)) and, finally, rinsed with Tris-buffered saline (TBS) completed with 0.1% Tween-20 (TBS-T, 50 mM Tris–HCl, 150 mM NaCl, pH 7.4). After its preincubation with a well blocked with the blocking buffer, the peptide library (2×10^{11} phages in 100 μl

Please cite this article in press as: Larbanoix, L., et al., Potential amyloid plaque-specific peptides for the diagnosis of Alzheimer's disease. Neurobiol. Aging (2008), doi:10.1016/j.neurobiolaging.2008.09.021

of TBS-T 0.1%) was incubated for 60 min at 37 °C with the target. After extensive rinsing of the well, phages bound to the target were eluted with 0.2 M glycin–HCl buffer (pH 2.2) completed with 0.1% BSA. Ten minutes later, the solution was neutralized with 1 M Tris–HCl buffer (pH 9.1). During the third and fourth rounds of biopanning, the selective pressure was enhanced by reducing the incubation time to 45 min and 30 min, respectively, and by increasing the Tween-20 concentration to 0.3% and 0.5%, respectively.

Between each round of biopanning, eluted phages were amplified by *Escherichia coli* (ER2738 host strain, New England Biolabs Inc.) infection. After amplification, the bacteria were removed by centrifugation and the phages were purified by serial precipitation with a solution of PEG/NaCl (20% PEG-8000, 2.5 M NaCl) at 4 °C. The phage pellet obtained by centrifugation was finally solubilized in TBS supplemented with 0.02% NaN_3.

The phage titer was determined after each round of biopanning and amplification by counting the blue plaques obtained after *E. coli* infection and growing on a selective medium containing isopropyl-beta-D-thiogalactoside (IPTG) (ICN Biomedical Inc., Brussels, Belgium) and 5-bromo-4-chloro-3-indolyl-beta-D-galactopyranoside (Xgal) (Sigma–Aldrich, Bornem, Belgium). The phage genome contains part of the LacZ gene that confers to bacteria the ability to produce β-galactosidase, which reacts with the X-gal substrate and results in a blue plaque staining.

2.2. Sequencing of selected phage clones

The phage single-strand DNA was isolated by the phenol/chloroform extraction procedure (Sambrook et al., 1989). The phage genome was sequenced by Sanger method using a 20-base primer (5′-CCCTCATAGTTAGCGTAACG-3′, New England Biolabs Inc.) located 96 nucleotides upstream to the inserted sequence. The DNA sequence was analyzed on a CEQ 2000 XL DNA Analysis System (Beckman Coulter™, Analis, Namur, Belgium). The sequence reading was performed automatically using the JaMBW 1.1 software (http://bioinformatics.org/JaMBW/).

2.3. Assaying the affinity of the selected phage clones for the target (ELISA)

$A\beta_{42}$ (10 μg/ml, 2.26 μM) was immobilized on ELISA plate that was subsequently blocked as described above in the protocol of biopanning. An additional number of microtiter wells were blocked in the absence of $A\beta_{42}$ to test the binding of the phage clones to BSA-coated plastic surface. Each well was incubated with 10^{12} phages in 100 μl TBS 2 h at 37 °C. The phage particles were detected with peroxidase conjugated anti-M13 monoclonal antibody (Amersham Pharmacia Biotech Benelux, Roosendaal, The Netherlands) diluted 1:5000 in the blocking buffer. The peroxidase staining reaction was developed in the presence of ABTS [2,2′-azino-bis(3-ethylbenz-tiazoline-6-sulfonic acid, diammonium salt), Sigma–Aldrich; 22 mg in 100 ml of 50 mM sodium citrate, pH 4.0] completed with 0.05% H_2O_2. After 30–60 min of incubation at room temperature, the OD_{405} values were measured on a microplate reader (Stat-Fax-2100, Awarness Technology Inc., Fisher Bioblock Scientific, Tournai, Belgium).

To determine the apparent dissociation constant (K_d^*), the $A\beta_{42}$ coated wells were incubated with twofold serial dilutions of each phage clone, starting with 10^{12} virions (1.66×10^{-8} M) in the first well and ending with 8×10^6 virions (1.33×10^{-13} M) in the last well.

2.4. Synthesis of biotinylated peptides

Peptides, and their scrambled homologous, were synthesized as 8-amino-3,6-dioxaoctanoyl derivatives and biotinylated (NeoMPS, Strasbourg, France).

2.5. Assaying the affinity of the selected peptides for $A\beta_{42}$ (ELISA)

To evaluate their K_d^* for $A\beta_{42}$, serial dilutions of biotinylated peptides ranging from 10^{-3} M to 10^{-6} M were incubated (2 h at 37 °C) with $A\beta_{42}$ immobilized on ELISA plate and blocked with a protein free blocking buffer (PFBB, Pierce, Aalst, Belgium). In order to assess the possible binding to other amyloidogenic peptides or proteins, and to prove thus the specific affinity to $A\beta_{42}$, control titration curves of biotinylated peptides were evaluated on amylin (or IAPP, Islet Amyloid PolyPeptide, Sigma–Aldrich) immobilized on ELISA plate at the same concentration as $A\beta_{42}$. The biotinylated peptides bound to the target were detected by incubation with 1 μg/ml of a goat anti-biotin antibody (Vector Laboratories, Brussels, Belgium) diluted in phosphate buffer (10 mM phosphate, 0.15 M NaCl). This was followed by incubation with 0.2 μg/ml of a peroxidase conjugated anti-goat antibody made in horse (Vector Laboratories) diluted in phosphate buffer supplemented with 0.1% Tween-20. After each incubation, the wells were washed with TBS-T 0.05%. The peroxidase staining reaction was developed with ABTS substrate solution.

2.6. Immunohistochemistry

2.6.1. Brain tissue preparation

The brain of $APP_{V717I}/PS1_{A246E}$ double transgenic mice (aged 22 months) (Experimental Genetics Group, KULeuven, Leuven, Belgium) was fixed for 24 h in 4% paraformaldehyde and embedded in paraffin. For immunohistochemistry of AP, brain sagittal sections (5 μm thick) were dewaxed, rehydrated and treated for 20 min with 70% formic acid. Sections were incubated successively with 0.15% H_2O_2 in PBS for 15 min, with endogenous biotin blocking kit (Invitrogen SA, Merelbeke, Belgium), and with PFBB for 1 h.

Please cite this article in press as: Larbanoix, L., et al., Potential amyloid plaque-specific peptides for the diagnosis of Alzheimer's disease. Neurobiol. Aging (2008), doi:10.1016/j.neurobiolaging.2008.09.021

2.6.2. Detection of AP with biotinylated peptides

The sections were incubated overnight with biotinylated peptides in TBS, followed by 5 μg/ml of goat anti-biotin IgG and 1 μg/ml of peroxidase-conjugated horse anti-goat IgG (60 min each). The staining was developed with 0.05% 3,3′-diaminobenzidine (DAB) and 0.02% H_2O_2 in PBS (phosphate-buffered saline buffer) after 5 min of incubation with 50 mM Tris–HCl pH 7.4. The sections were finally counterstained with Meyer's hemalun and mounted in a permanent medium.

2.6.3. Detection of AP with anti-A$\beta_{17–24}$ antibody 4G8

The brain sections were incubated overnight with 1 μg/ml monoclonal antibody 4G8 (Abcam, Cambridge, UK) followed by 4 μg/ml of peroxidase conjugated rat anti-mouse secondary antibody (Sigma–Aldrich) (1 h at room temperature). The following steps were similar to the protocol described above.

2.6.4. Detection of AP with thioflavin-S

The brain sections were rehydrated and directly incubated 30 min with 0.01% thioflavin-S in 50% ethanol. Sections were then washed in 50% ethanol and in distilled water and finally mounted in Vectashield media (Vector Laboratories).

2.6.5. Detection of AP with PHO conjugated to ultrasmall particles of iron oxide (USPIO–PHO)

Sections were incubated 2 h with USPIO–PHO (30.4 mM of iron; see below USPIO–PHO preparation) or with control USPIO and then the iron was stained by Perl's method (Prussian blue). A counter-staining was performed with Sirius Red to localize the AP.

2.7. Preliminary in vivo evaluation of PHO linked to an MRI contrast agent

2.7.1. Conjugation of PHO to USPIO

The peptide was linked covalently to USPIO in two steps: the reactive alkyl halogen end of epichlohydrin was first coupled to the hydroxyls of dextran coating of Fe_3O_4 particles to obtain a terminal glycidyl ether derivative which was then used to link the amine group of the peptide. Longitudinal (r_1) and transverse (r_2) relaxivities (NMR efficiency expressed in s^{-1} mM^{-1}) of USPIO–PHO were measured at 37 °C and 20 MHz ($r_1 = 32.26$, $r_2 = 85.32$ and $r_2/r_1 = 2.64$) and 60 MHz ($r_1 = 13.50$, $r_2 = 83.75$ and $r_2/r_1 = 6.20$).

2.7.2. Molecular imaging by MRI

USPIO–PHO was administrated i.v. to a 22 months old double transgenic mouse $APP_{V717I}/PS1_{A246E}$ at a dose of 80 μmol Fe/kg. To open the blood–brain barrier (BBB), the mice were first injected i.v. with a solution of 25% mannitol (14 ml/kg). A wild type (WT) control mouse received the same treatment. T_2 weighted images were acquired on a 4.7 T Bruker Avance-200 imaging system (Bruker, Karlsruhe, Germany) (Micro2.5AHS/RF, 25 mm coil) by using a RARE sequence (TR/TE = 5552/68 ms, NE = 32, matrix 128 × 128, slice thickness = 1.5 mm, FOV = 2.5 cm, spatial resolution = 195 μm). Signal intensity (SI) values for each time delay were measured by drawing regions of interest globally within the brain, as well as in an area located outside the head's image to define the noise level. The percentage enhancement of signal/noise was calculated as the ratio of the difference between pre- and post-contrast SI to pre-contrast SI.

2.7.3. Blood pharmacokinetics and biodistribution of USPIO–PHO

Blood pharmacokinetics of USPIO–PHO and of USPIO were assessed on male Wistar rats after a single i.v. injection of 0.1 mmol Fe/kg bw. The iron content of blood samples was determined by relaxometry at 60 MHz on a Bruker mq60 Minispec. A two-compartment distribution model was used to calculate the pharmacokinetic parameters such as the elimination half-life ($T_{e1/2}$), the volume of steady state distribution (VD_{ss}), and the total clearance (Cl_{tot}). The apparent biodistribution was determined in rats 2 h after contrast agent administration. Iron content was evaluated by relaxometry at 10 MHz on a Bruker minispec PC-110 (Bruker). Transverse relaxation rate (R_2) values ($1/T_2$) were computed and normalized compared to organs of no treated rats (R_2^{Norm}).

The mean ± S.E.M. were calculated for each experimental group and the statistical significance was evaluated with Student's t test. The results were considered as significant for a $p < 0.05$.

2.7.4. Evaluation of USPIO–PHO binding affinity by NMR relaxometry

To evaluate the K_d^* for $A\beta_{42}$ interaction, serial dilutions of $A\beta_{42}$ ranging from 10^{-7} M to 10^{-16} M were incubated (3 min

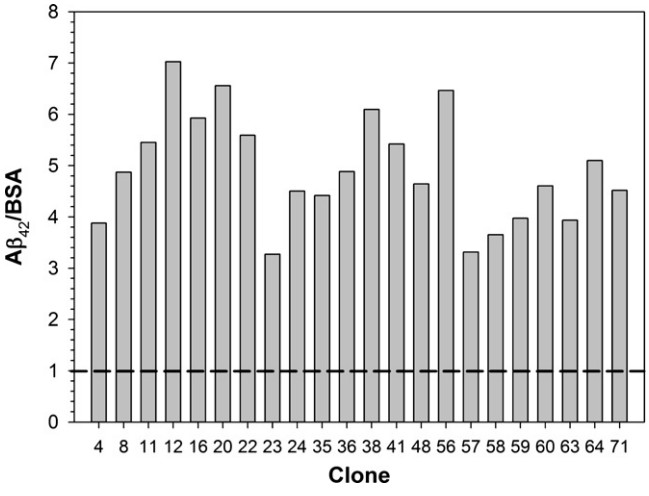

Fig. 1. Affinity of the 22 selected clones for $A\beta_{42}$ and BSA as evaluated by ELISA. The results, expressed as a ratio between the two affinities, show 3–7 times higher affinity for $A\beta_{42}$ than for BSA. The phage clones were selected after four rounds of biopanning and their affinity was assessed at a concentration of 10^{13} virions/ml (1.66×10^{-8} M).

Please cite this article in press as: Larbanoix, L., et al., Potential amyloid plaque-specific peptides for the diagnosis of Alzheimer's disease. Neurobiol. Aging (2008), doi:10.1016/j.neurobiolaging.2008.09.021

at 37 °C) with 25 μM USPIO–PHO, and, as control, with 25 μM USPIO. Then, T_2 relaxation time was measured on a Bruker mq60 relaxometer (60 MHz) and the percentage effect (% effect) of $A\beta_{42}$ on R_2 of USPIO–PHO was calculated by relating it to R_2 of contrast agent alone.

3. Results

3.1. Affinity for $A\beta_{42}$ of the selected phage clones

Seventy-two clones were isolated arbitrarily from the output of the fourth round of panning. Their individual affinities were evaluated and 22 clones showed the most important specific affinity for $A\beta_{42}$ as compared to that for BSA (Fig. 1). These clones were selected for further characterization.

3.2. Amino acid sequence of the selected peptides

The DNA of the 22 clones selected on the basis of their affinity for $A\beta_{42}$ was sequenced and 12 peptide inserts were identified (Fig. 2A). The library has been enriched in two sequences after four rounds of biopanning, C-IPLPFYN-C and C-FRHMTEQ-C, respectively. Their amino acid composition is prevalently hydrophobic or hydrophilic, respectively, which indicates different mechanisms of interaction with $A\beta_{42}$. The library has been also lightly enriched in a third sequence, C-SHLYLHN-C. Another clone possesses a peptide (C-IPLLFHN-C) that differs by two amino acids (P4H and Y6H) from the highly selected C-IPLPFYN-C. It is well known that a minimal structure modification can lead to a change of conformation or to other physico-chemical alterations that can be associated with a change of affinity for the target.

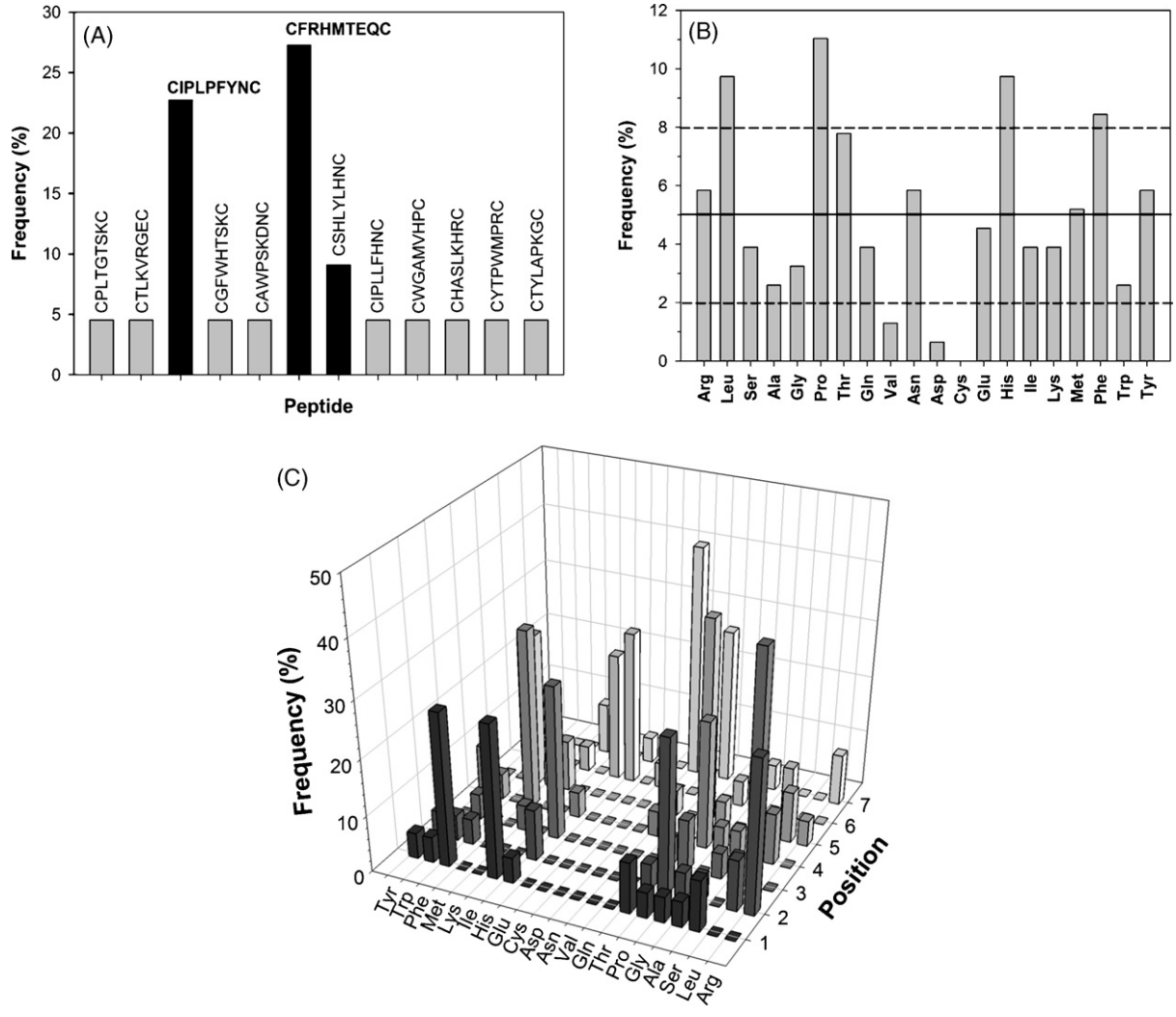

Fig. 2. Amino acid sequence of peptides displayed by the 22 selected phage clones. (A) Frequency of peptides displayed by the phage clones. Two sequences were highly represented, C-IPLPFYN-C and C-FRHMTEQ-C; sequence C-SHLYLHN-C was also frequent, although to a lesser extent. (B) Amino acid frequency in the heptapeptides displayed by the selected clones. The solid line shows the mean value while the dotted line indicates the variance. Globally, hydrophobic amino acids, such as Phe, Pro and Leu, are the most frequent in these 22 clones. (C) Frequency representation of amino acids in each position of the heptapeptide sequences. In each position, there are 2 or 3 amino acids that are highly represented.

Please cite this article in press as: Larbanoix, L., et al., Potential amyloid plaque-specific peptides for the diagnosis of Alzheimer's disease. Neurobiol. Aging (2008), doi:10.1016/j.neurobiolaging.2008.09.021

The amino acid frequency in the peptide structures is represented in Fig. 2B. Among all amino acids, only cystein is absent. In fact, cystein is rarely present in the displayed peptides because it can diminish the phage infectivity by forming disulfide links. The other 19 amino acids are present in a rather homogenous way, but some of them are overexpressed like Leu, Pro, His, and Phe, suggesting that a hydrophobic type of binding was favored during the selection protocol. The amino acid position in the inserts is shown in Fig. 2C. Interestingly, at each position, there are two or three amino acids that are highly represented. More often, they are hydrophobic (Ile, Phe, Pro, Leu and Met) but also basic (Arg and His) and with a hydroxyl function (Thr and Tyr).

3.3. K_d^* of the selected clones for $A\beta_{42}$

The K_d^* values were estimated for the 12 different clones with the aim of identifying the most efficient ones (Fig. 3A). All clones have K_d^* values lower than 10^{-9} M, with the exception of one which has a K_d^* of 2×10^{-9} M. Clone HO (C-IPLPFYN-C) and clone HI (C-FRHMTEQ-C), which display the two strongly selected peptide sequences, have K_d^* values in the picomolar range (2.2×10^{-10} M and 5.45×10^{-10} M, respectively). Consequently, their peptides (PHO and PHI) were synthesized, biotinylated (PHOb and PHIb, respectively), and characterized *in vitro*. To confirm their specific binding to the target, their scramble derivatives (PHOb-Sc and PHIb-Sc) were also synthesized and characterized.

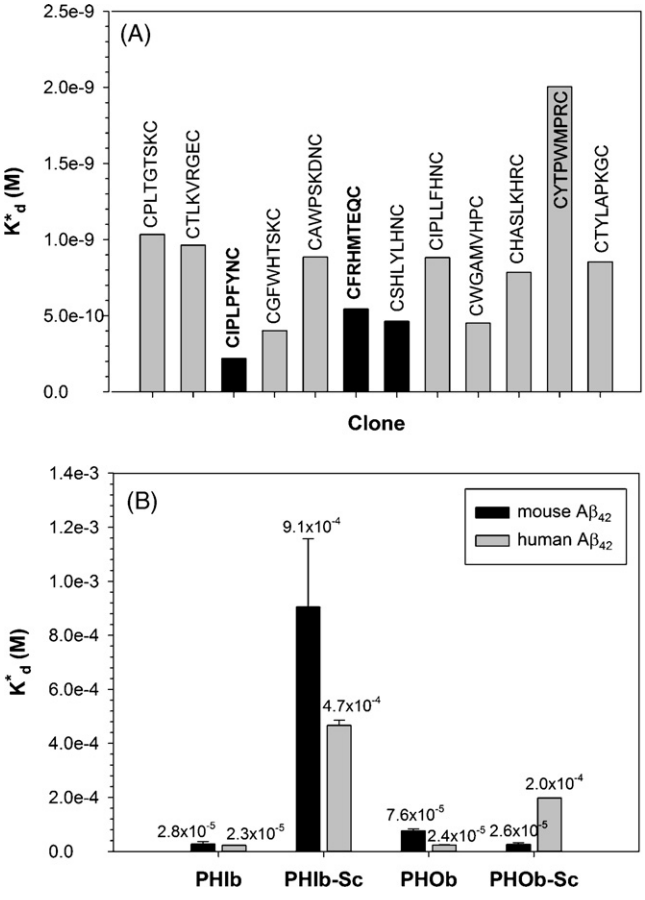

Fig. 3. K_d^* values of the selected phage clones and of the corresponding biotinylated peptides as determined by ELISA. (A) K_d^* of the 12 selected clones displaying the highest affinities for $A\beta_{42}$. C-IPLPFYN-C, C-FRHMTEQ-C and C-SHLYLHN-C have a K_d^* of 2.2×10^{-10} M, 5.45×10^{-10} M and 4.64×10^{-10} M, respectively. (B) K_d^* of the two selected peptides, PHIb and PHOb, for mouse and human $A\beta_{42}$. The diminished affinity of PHIb-Sc suggests that the PHI sequence is essential for its interaction with $A\beta_{42}$.

3.4. K_d^* of the biotinylated peptides for $A\beta_{42}$

The K_d^* of biotinylated peptides were evaluated on mouse and human $A\beta_{42}$ (Fig. 3B). K_d^* values show a better affinity for mouse and human $A\beta_{42}$ of PHIb ($K_d^* = 2.80 \times 10^{-5}$ M and 2.25×10^{-5} M, respectively) than of PHIb-Sc ($K_d^* = 9.05 \times 10^{-4}$ M and 4.67×10^{-4} M, respectively). The loss of binding affinity of PHIb-Sc confirms that the PHIb sequence is important for its specific interaction with $A\beta_{42}$. PHOb has more affinity for human $A\beta_{42}$ ($K_d^* = 2.41 \times 10^{-5}$ M) than for mouse $A\beta_{42}$ ($K_d^* = 7.61 \times 10^{-5}$ M). The K_d^* of PHOb-Sc indicates an even stronger interaction with mouse $A\beta_{42}$ ($K_d^* = 2.61 \times 10^{-5}$ M) than that of PHOb, but it loses its affinity for human $A\beta_{42}$ ($K_d^* = 1.98 \times 10^{-4}$ M). Thus, it seems that these peptides interact with $A\beta_{42}$ thanks to their hydrophobic properties and thus they are less sensitive to the amino acid sequence than PHI and PHI-Sc. The possible affinity for other amyloidogenic peptides or proteins was assessed by taking amylin as an example, which is a molecule associated with type 2 diabetes (Haataja et al., 2008). Neither PHIb nor PHOb present any affinity for amylin (data not shown), which proves their specificity for $A\beta_{42}$.

3.5. Validation of AP binding by the selected peptides

To confirm the specific binding to AP, sagittal sections of APP/PS1 mouse brain were stained with 20 μM biotinylated peptides. The specificity of this distribution was confirmed on serial sections by using a monoclonal anti-Aβ antibody (clone 4G8) and thioflavin-S. A peripheral staining of AP was observed in cortex (Fig. 4), as well as in hippocampus, in striatum, olfactory bulb, and thalamus (data not shown). The staining appeared quite similar for PHOb (Fig. 4A) and PHOb-Sc (Fig. 4J). PHIb allowed the staining of AP at a lower concentration (1 μM, Fig. 4J) as opposed to the other peptides (see PHIb-Sc, Fig. 4M). Peptides seem to stain more the periphery of senile plaques and the diffuse AP than the dense core of senile plaques. Indeed, the presence of diffuse deposits is confirmed by staining with 4G8 antibody. On the contrary, thioflavin-S stained only the dense core of senile plaques (Fig. 4B, E and H). The secondary antibodies used for revelation of biotinylated peptides and of 4G8 antibody were not responsible for these staining variations as demonstrated by negative controls (Fig. 4K and N, respectively).

Please cite this article in press as: Larbanoix, L., et al., Potential amyloid plaque-specific peptides for the diagnosis of Alzheimer's disease. Neurobiol. Aging (2008), doi:10.1016/j.neurobiolaging.2008.09.021

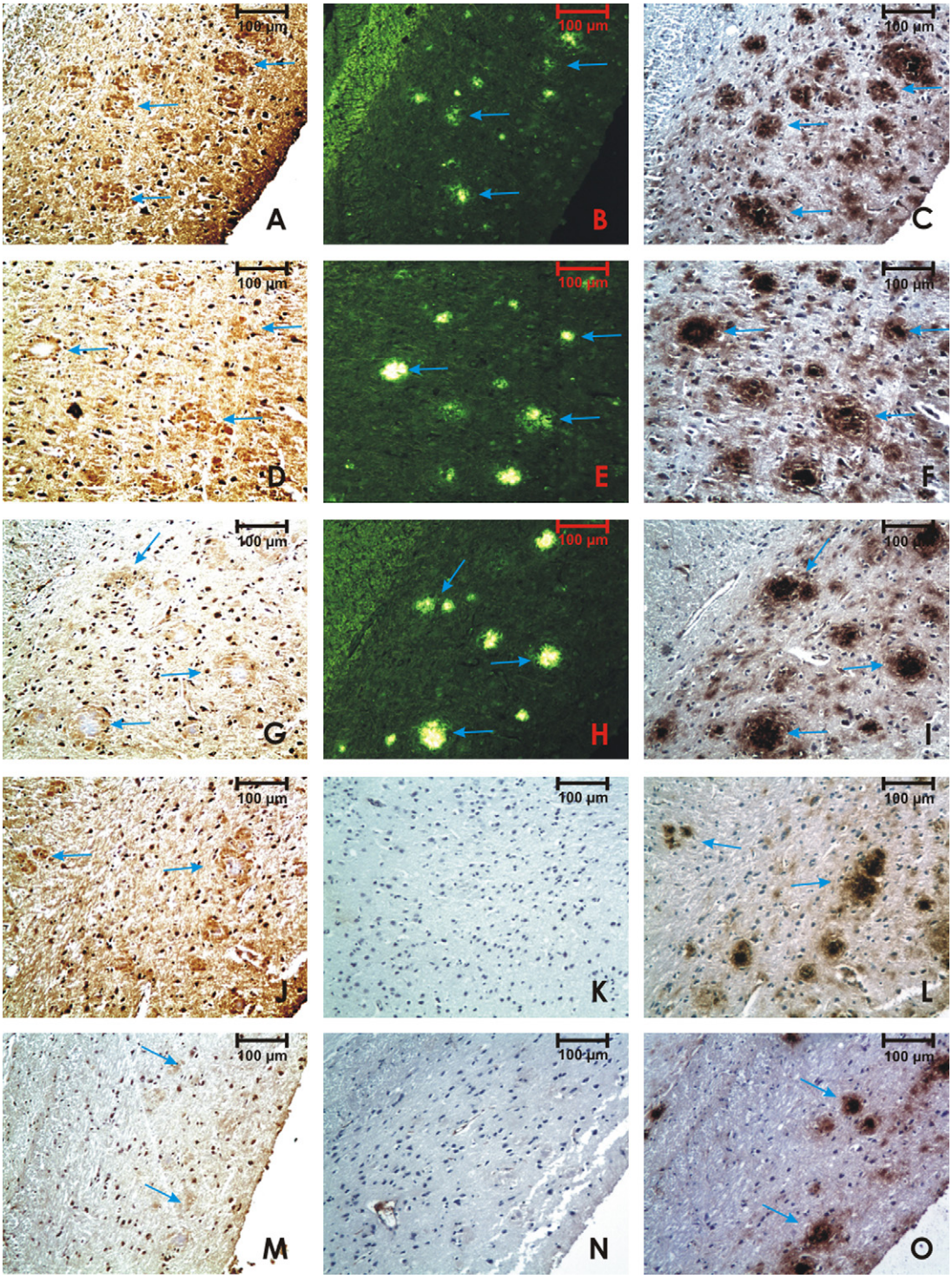

Fig. 4. Amyloid plaque staining with 20 µM PHOb (A), 20 µM PHIb (D), 1 µM PHIb (G), 20 µM PHOb-Sc (J) and 1 µM PHIb-Sc (M) and co-localization with thioflavin-S (B, E and H) and 4G8 antibody (C, F, I, L and O) in serial sections of an APP/PS1 mouse brain showed in cortex. Pictures (A–C), (D–F), and (G–I) show the same area on successive slices separated by 5 µm. Peptides stained diffuse plaques and neuritic plaques, but the cores of senile plaques appeared less stained. Thioflavin-S and 4G8 antibody confirm the nature of amyloid plaques. Neuritic plaques with dense core were highly stained with thioflavin-S and appeared as intense yellow areas, whereas diffuse plaques were slightly stained. 4G8 allows the visualization of both diffuse plaques and of neuritic plaques. Pictures (J) and (L), and pictures (M) and (O) show the same area on successive slices separated by 5 µm and 10 µm, respectively. Negative controls of peptides and of 4G8 are not showing any staining (K and N, respectively).

Please cite this article in press as: Larbanoix, L., et al., Potential amyloid plaque-specific peptides for the diagnosis of Alzheimer's disease. Neurobiol. Aging (2008), doi:10.1016/j.neurobiolaging.2008.09.021

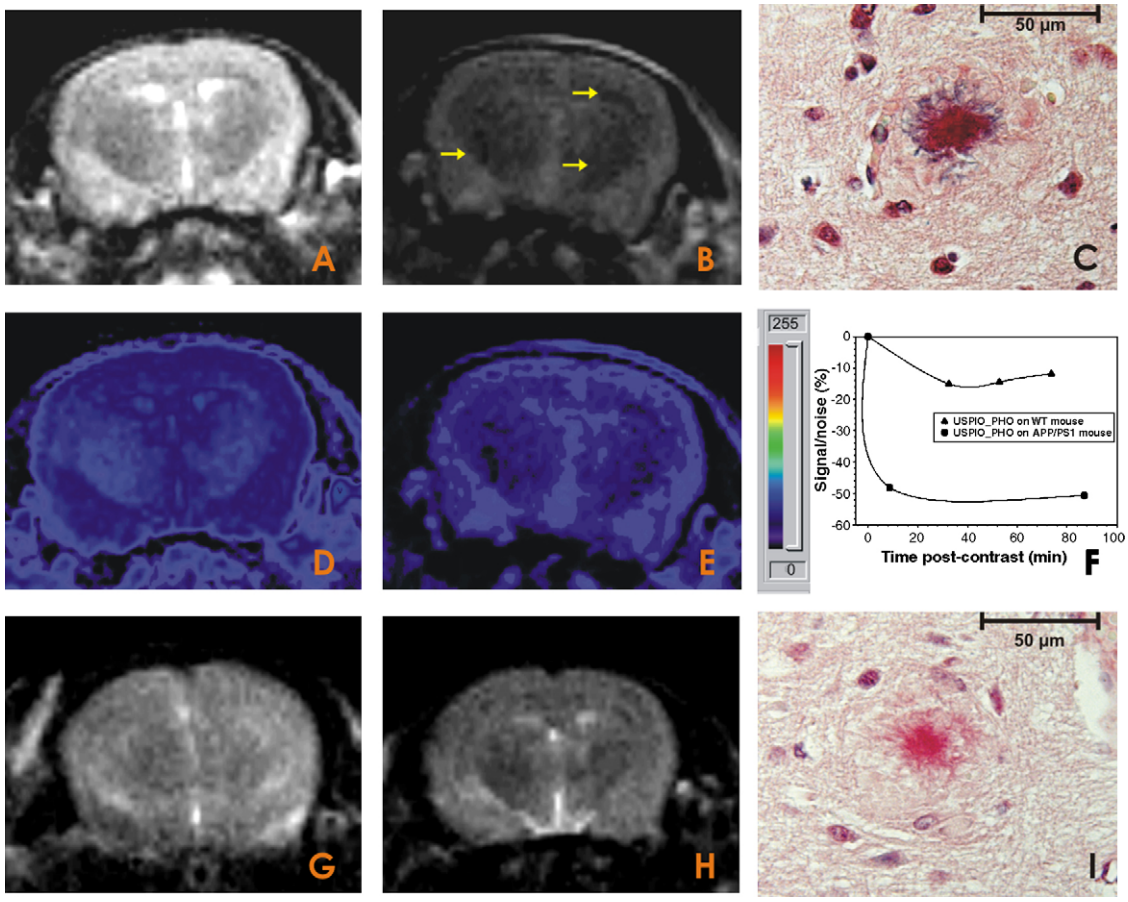

Fig. 5. Molecular imaging of AP with USPIO–PHO by using a T_2-weighted MRI sequence in a 22 months old double $APP_{V717I}/PS1_{A246E}$ transgenic mouse (A and B) and in a control mouse (G and H): pre-contrast MR images (A and G) and 1h30 post-contrast MR images (B and H) are shown. (D) and (E) are color overlay of (A) and (B). USPIO–PHO are located in the cortex and striatum/thalamic area (B and E). There is a high contrast effect in the APP/PS1 mouse, but not in the WT mouse brain as shown by the signal/noise ratio of brain in MR images (F) after administration of USPIO–PHO. Binding of USPIO–PHO to amyloid plaques was confirmed by Perl's iron staining method on sagittal sections of APP/PS1 mouse brain (C); this was indicated by the blue staining around the red labeled core of plaques after Sirius Red counter-staining. Not functionalized USPIO did not bind to the plaques (I).

In conclusion, these observations confirm the binding affinities already demonstrated by ELISA and suggest that these peptides could be effective tools to detect AP by an imaging methodology.

3.6. *In vivo MRI evaluation of USPIO–PHO*

To assess molecular imaging of AP with a contrast agent functionalized by one of the two selected peptides, MRI was performed *in vivo* on APP/PS1 transgenic mouse before and after the injection of USPIO-PHO and the opening of BBB with 25% mannitol. A significant decrease of signal intensity was produced by USPIO–PHO in the brain of APP/PS1 mouse, particularly in the cortex and striatum areas (Fig. 5A, B, D and E), but not in the brain of WT mouse (Fig. 5G and H). The measurement of percentage enhancement of signal/noise (Fig. 5F) indicates its decrease to −48% 9 min after USPIO–PHO injection to APP/PS1 mouse, and this was constant until the end of the imaging session (87 min). In WT mouse, the lowest signal decrease (−15%) was observed 32 min post-contrast.

3.7. *Validation of the affinity for AP of USPIO–PHO by histochemistry*

To confirm the affinity for AP of USPIO–PHO, APP/PS1 mouse brain sections were stained for iron after incubation with USPIO or with USPIO–PHO. The peripheral area of AP is stained in blue in the sample incubated with USPIO–PHO, but not in that incubated with USPIO (Fig. 5C and I). The core of neuritic plaques appeared red thanks to Sirius Red counter-staining. These results confirm the specific binding of USPIO–PHO to AP.

3.8. *Evaluation of blood pharmacokinetics and of apparent biodistribution of USPIO–PHO*

The pharmacokinetic profiles show that USPIO–PHO are eliminated from blood at a much slower rate than USPIO

Please cite this article in press as: Larbanoix, L., et al., Potential amyloid plaque-specific peptides for the diagnosis of Alzheimer's disease. Neurobiol. Aging (2008), doi:10.1016/j.neurobiolaging.2008.09.021

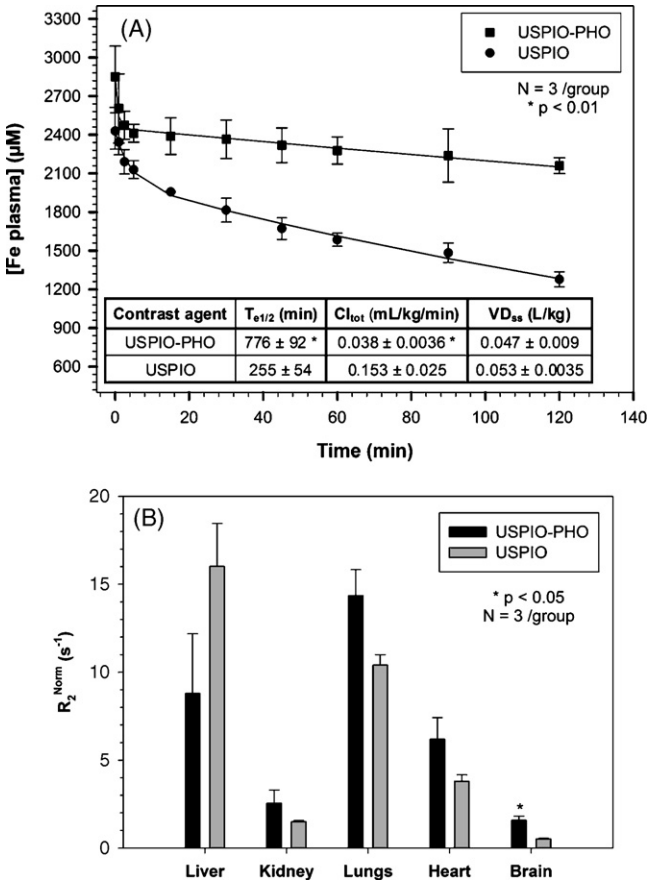

Fig. 6. (A) Pharmacokinetic parameters of USPIO–PHO and USPIO performed on healthy Wistar rats. USPIO–PHO is eliminated from blood much slowly than USPIO. (B) Apparent USPIO–PHO and USPIO biodistributions evaluated on healthy Wistar rats 2 h after administration. Both contrast agents are accumulated in liver and lungs, whereas brain accumulated significantly more USPIO–PHO than USPIO.

(Fig. 6A). Indeed, USPIO–PHO has a longer elimination half-life and a slower total clearance than USPIO.

The major part of iron is found in lungs and liver (Fig. 6B). There is a significant enrichment of USPIO–PHO in the brain as compared to USPIO ($p < 0.05$).

3.9. Characterization of USPIO–PHO by NMR relaxometry

The molecular interaction between mouse $A\beta_{42}$ and USPIO–PHO was measured by NMR relaxometry (Fig. 7), which was sensitive and directly proportional to the variation of $A\beta_{42}$ concentration. The saturation curve obtained in these conditions was used to estimate the K_d^* value (1.2×10^{-10} M), which was comparable to that obtained for the corresponding phage clone. This result suggests that polyvalent exposure of peptides on the surface of iron particles reproduces the avidity effect of phages or that NMR relaxometry is more sensitive than ELISA. No significant modification of the relaxation time was observed for control

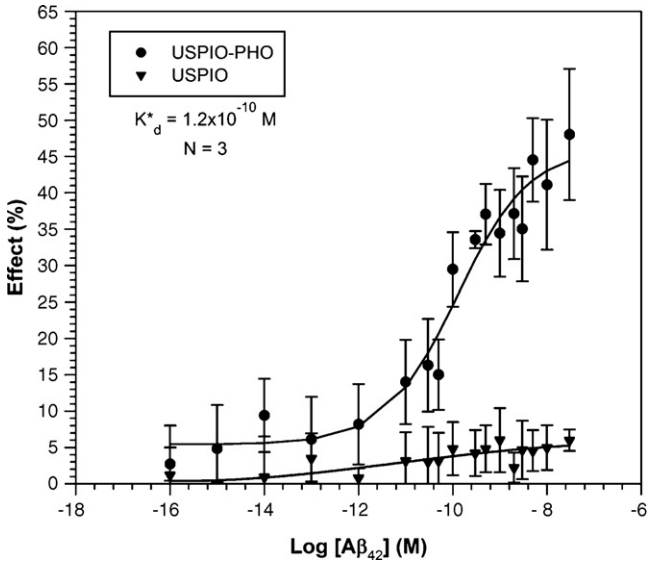

Fig. 7. K_d^* of USPIO–PHO for mouse $A\beta_{42}$ as determined by NMR relaxometry. As a negative control, USPIO does not show any affinity for mouse $A\beta_{42}$.

USPIO, which does not interact with $A\beta_{42}$, and thus confirms the specific interaction between USPIO–PHO and $A\beta_{42}$.

4. Discussion

Diagnosis of AD in living patients remains problematic and is mainly based on cognitive tests. In particular, clinicians need additional and reliable methods to detect the pathologic manifestations of the disease well before the first symptoms of dementia. In this context, molecular imaging techniques, like MRI, PET, and SPECT, are very promising and potential tools able of both detecting AD-related biomarkers such as AP and also of monitoring the evolution of this pathology. The technique of phage display was applied in the present work with the aim of searching for peptide ligands able to vectorize an AP-targeted contrast agent. In this study, 12 different peptides, identified from a total of 22 sequenced phage clones, displayed a high affinity for $A\beta_{42}$, the main component of AP. Two phage clones expressing the peptides C-IPLPFYN-C and C-FRHMTEQ-C were strongly selected because they are present in several copies and are characterized by K_d^* values in the picomolar range, i.e. 2.2×10^{-10} M and 5.45×10^{-10} M, respectively. The first peptide is characterized by five hydrophobic amino acids out of seven suggesting that it interacts with $A\beta_{42}$ by hydrophobic bonds. It is interesting to note that $A\beta_{42}$ itself aggregates by hydrophobic mechanisms inside AP structures. On the other hand, peptide C-FRHMTEQ-C is hydrophilic, so the interaction mechanism should be different and could involve the hydrophilic N-terminus domain of $A\beta_{42}$.

After synthesis and biotinylation, the binding affinities of peptides fell in the micromolar range probably as a conse-

Please cite this article in press as: Larbanoix, L., et al., Potential amyloid plaque-specific peptides for the diagnosis of Alzheimer's disease. Neurobiol. Aging (2008), doi:10.1016/j.neurobiolaging.2008.09.021

quence of their monovalent presentation, which is known to have dramatic consequences on binding affinities. Indeed, the polyvalent exposure of peptides inserted in the phage capside leads to an avidity effect (Clackson and Lowman, 2004). Nevertheless, these affinity values remain compatible with clinical MRI applications for which contrast agents are usually injected at a dose of 0.1 mmol/kg for diagnosis. Contrast agents could also be designed to expose peptides in a polyvalent format by conjugation to dendrimers (Bryant et al., 1999) or to nanoparticles of iron oxide (Zhao et al., 2002).

As the peptides were selected on mouse $A\beta_{42}$, but are destined for human AP detection, their K_d^* were evaluated both on mouse and on human $A\beta_{42}$. Peptide HI (C-FRHMTEQ-C) has quite the same affinity for mouse and human $A\beta_{42}$, while peptide HO (C-IPLPFYN-C) has a better affinity for human $A\beta_{42}$. The affinity for $A\beta_{42}$ of biotinylated peptide HI is lost when its sequence is modified, a fact that confirms the specific interaction with $A\beta_{42}$. On the contrary, the biotinylated peptide HO has an improved affinity for mouse $A\beta_{42}$ but loses it for human $A\beta_{42}$ in a scramble presentation. Moreover, the specific interaction of peptides HI and HO with $A\beta_{42}$ is confirmed by the absence of any affinity for amylin, another amyloidogenic peptide that is involved in type 2 diabetes. PHI presents the advantage of a high solubility, while PHO is able to cross more easily cellular membranes as a consequence of its hydrophobicity. The histological examination of biotinylated peptides interacting with AP in mouse brains confirms their targeting potential.

The preliminary studies performed with USPIO–PHO are encouraging by showing higher retention of AP-targeted contrast agent in the brain of transgenic mouse than in the brain of healthy mouse. Moreover, the binding capacity to AP and to $A\beta_{42}$ of our contrast agent was confirmed by histochemistry and by NMR relaxometry, respectively.

In conclusion, our results indicate that these peptides are good candidates to design contrast agents dedicated to the *in vivo* AP imaging. However, the passage of the BBB remains the first limiting factor for any brain targeting drugs. In this context, different strategies could be applied to facilitate diffusion across this biological barrier, such as polyamine derivatization of the vector molecule (Poduslo et al., 2004), osmotic shock with mannitol (Wadghiri et al., 2003), or the carrying by polysorbate coated nanoparticles (Kreuter, 2001).

Disclosure statement

Lionel Larbanoix: none; Carmen Burtea: none; Sophie Laurent: none; Fred Van Leuven: none; Gérard Toubeau: none; Luce Vander Elst: none; Robert N. Muller: none.

Conflict of interest

There is no conflict of interest declared.

Acknowledgments

FRIA, ARC (no. 05-10/335), EMIL NoE (EU), NOMADE project.

The authors thank Mrs Patricia de Francisco for her help in preparing the manuscript and Mrs Annik Maes for her help in preparing histological material.

References

Benveniste, H., Einstein, G., Kim, K.R., Hulette, C., Johnson, A., 1999. Detection of neuritic plaques in Alzheimer's disease by magnetic resonance microscopy. Proc. Natl. Acad. Sci. U.S.A. 96 (24), 14079–14084.

Borthakur, A., Gur, T., Wheaton, A.J., Corbo, M., Trojanowski, J.Q., Lee, V.M.-Y., Reddy, R., 2006. In vivo measurement of plaque burden in a mouse model of Alzheimer's disease. MRI 24, 1011–1017.

Boutry, S., Burtea, C., Laurent, S., Toubeau, G., Vander Elst, L., Muller, R.N., 2005. Magnetic resonance imaging of inflammation with a specific selectin-targeted contrast agent. Magn. Reson. Med. 53 (4), 800–807.

Brass, S.D., Chen, N.K., Mulkern, R.V., Bakshi, R., 2006. Magnetic resonance imaging of iron deposition in neurological disorders. Top. Magn. Reson. Imaging 17 (1), 31–40.

Bryant, L.H., Brechbiel, M.W., Wu, C.C., Bulte, J.W.M., Herynek, V., Frank, J.A., 1999. Synthesis and relaxometry of high-generation (G = 5, 7, 9, and 10) PAMAM dendrimer-DOTA-gadolinium chelates. J. Magn. Reson. Imaging 9 (2), 348–352.

Burtea, C., Laurent, S., Murariu, O., Rattat, D., Toubeau, G., Verbruggen, A., Vansthertem, D., Vander, E.L., Muller, R.N., 2008. Molecular imaging of $\alpha_v\beta_3$ integrin expression in atherosclerotic plaques with a mimetic of RGD peptide grafted to Gd-DTPA. Cardiovasc. Res. 78 (1), 148–157.

Clackson, T., Lowman, H.B., 2004. Phage Display: Practical Approach. Oxford University Press Inc., New York.

Dhenain, M., El Tannir El, T.N., Wu, T.D., Guegan, M., Volk, A., Quintana, C., Delatour, B., 2007. Characterization of in vivo MRI detectable thalamic amyloid plaques from APP/PS1 mice. Neurobiol. Aging, doi:10.1016/j.neurobiolaging.2007.05.018.

Haataja, L., Gurlo, T., Huang, C.J., Bulter, P.C., 2008. Islet amyloid in type 2 diabetes, and the toxic oligomer hypothesis. Endocr. Rev. 29 (3), 303–316.

Hartmann, T., Bieger, S.C., Bruhl, B., Tienari, P.J., Ida, N., Allsop, D., Roberts, G.W., Masters, C.L., Dotti, C.G., Unsicker, K., Beyreuther, K., 1997. Distinct sites of intracellular production for Alzheimer's disease A beta 40/42 amyloid peptides. Nat. Med. 3 (9), 1016–1020.

Higuchi, M., Iwata, N., Matsuba, Y., Sato, K., Sasamoto, K., Saido, T.C., 2005. F-19 and H-1 MRI detection of amyloid beta plaques in vivo. Nat. Neurosci. 8 (4), 527–533.

Huang, X.D., Atwood, C.S., Hartshorn, M.A., Multhaup, G., Goldstein, L.E., Scarpa, R.C., Cuajungco, M.P., Gray, D.N., Lim, J., Moir, R.D., Tanzi, R.E., Bush, A.I., 1999. The A beta peptide of Alzheimer's disease directly produces hydrogen peroxide through metal ion reduction. Biochemistry 38 (24), 7609–7616.

Iversen, L.L., Mortishiresmith, R.J., Pollack, S.J., Shearman, M.S., 1995. The toxicity in-vitro of beta-amyloid protein. Biochem. J. 311, 1–16.

Jack, C.R., Garwood, M., Wengenack, T.M., Borowski, B., Curran, G.L., Lin, J., Adriany, G., Grohn, I.H.J., Grimm, R., Poduslo, J.F., 2004. In vivo visualization of Alzheimer's amyloid plaques by magnetic resonance imaging in transgenic mice without a contrast agent. Magn. Reson. Med. 52 (6), 1263–1271.

Jagust, W., Reed, B., Mungas, D., Ellis, W., Decarli, C., 2007. What does fluorodeoxyglucose PET imaging add to a clinical diagnosis of dementia? Neurology 69 (9), 871–877.

Kang, C.K., Jayasinha, V., Martin, P.T., 2003. Identification of peptides that specifically bind A beta(1–40) amyloid in vitro and amyloid plaques in

Alzheimer's disease brain using phage display. Neurobiol. Dis. 14 (1), 146–156.

Kreuter, J., 2001. Nanoparticulate systems for brain delivery of drugs. Adv. Drug Deliv. Rev. 47 (1), 65–81.

Lee, S.P., Falangola, M.F., Nixon, R.A., Duff, K., Helpern, J.A., 2004. Visualization of beta-amyloid plaques in a transgenic mouse model of Alzheimer's disease using MR microscopy without contrast reagents. Magn. Reson. Med. 52 (3), 538–544.

Nordberg, A., 2008. Amyloid plaque imaging in vivo: current achievement and future prospects. Eur. J. Nucl. Med. Mol. Imaging 35 (s1), s46–s50.

Orner, B.P., Liu, L., Murphy, R.M., Kiessling, L.L., 2006. Phage display affords peptides that modulate beta-amyloid aggregation. J. Am. Chem. Soc. 128 (36), 11882–11889.

Poduslo, J.F., Curran, G.L., Peterson, J.A., McCormick, D.J., Fauq, A.H., Khan, M.A., Wengenack, T.M., 2004. Design and chemical synthesis of a magnetic resonance contrast agent with enhanced in vitro binding, high blood–brain barrier permeability, and in vivo targeting to Alzheimer's disease amyloid plaques. Biochemistry 43 (20), 6064–6075.

Rapoport, M., Ferreira, A., 2000. PD98059 prevents neurite degeneration induced by fibrillary beta-amyloid in mature hippocampal neurons. J. Neurochem. 74 (1), 125–133.

Rogers, J., Lue, L.F., 2001. Microglial chemotaxis, activation, and phagocytosis of amyloid beta-peptide as linked phenomena in Alzheimer's disease. Neurochem. Int. 39 (5/6), 333–340.

Sambrook, J., Fritsch, E.F., Maniatis, T., 1989. Molecular Cloning: A Laboratory Manual. Cold Spring Harbor Laboratory Press, New York.

Segers, J., Laumonier, C., Burtea, C., Laurent, S., Elst, L.V., Muller, R.N., 2007. From phage display to magnetophage, a new tool for magnetic resonance molecular imaging. Bioconjug. Chem. 18 (4), 1251–1258.

Sigurdsson, E.M., Wadghiri, Y.Z., Mosconi, L., Blind, J.A., Knudsen, E., Asuni, A., Scholtzova, H., Tsui, W.H., Li, Y., Sadowski, M., Turnbull, D.H., de Leon, M.J., Wisniewski, T., 2007. A non-toxic ligand for voxel-based MRI analysis of plaques in AD transgenic mice. Neurobiol. Aging, doi:10.1016/j.neurobiolaging.2006.12.018.

Sipe, J.D., 2005. Amyloid Proteins. The Beta Sheet Conformation and Disease. WILEY-VCH, New York.

Smith, G.P., Petrenko, V.A., 1997. Phage display. Chem. Rev. 97 (2), 391–410.

Van Dorpe, J., Smeijers, L., Dewachter, I., Nuyens, D., Spittaels, K., Van den Haute, C., Mercken, M., Moechars, D., Laenen, I., Kuiperi, C., Bruynseels, K., Tesseur, I., Loos, R., Vanderstichele, H., Checler, F., Sciot, R., Van Leuven, F., 2000. Prominent cerebral amyloid angiopathy in transgenic mice overexpressing the London mutant of human APP in neurons. Am. J. Pathol. 157 (4), 1283–1298.

Vanhoutte, G., Dewachter, I., Borghgraef, P., Van Leuven, F., Van der Linden, A., 2005. Noninvasive in vivo MRI detection of neuritic plaques associated with iron in APP[V717I] transgenic mice, a model for Alzheimer's disease. Magn. Reson. Med. 53 (3), 607–613.

Wadghiri, Y.Z., Sigurdsson, E.M., Sadowski, M., Elliott, J.I., Li, Y.S., Scholtzova, H., Tang, C.Y., Aguinaldo, G., Pappolla, M., Duff, K., Wisniewski, T., Turnbull, D.H., 2003. Detection of Alzheimer's amyloid in transgenic mice using magnetic resonance microimaging. Magn. Reson. Med. 50 (2), 293–302.

Weissleder, R., Mahmood, U., 2001. Molecular imaging. Radiology 219 (2), 316–333.

Wiesehan, K., Buder, K., Linke, R.P., Patt, S., Stoldt, M., Unger, E., Schmitt, B., Bucci, E., Willbold, D., 2003. Selection of D-amino-acid peptides that bind to Alzheimer's disease amyloid peptide A beta(1–42) by mirror image phage display. Chembiochem 4 (8), 748–753.

Zhao, M., Kircher, M.F., Josephson, L., Weissleder, R., 2002. Differential conjugation of tat peptide to superparamagnetic nanoparticles and its effect on cellular uptake. Bioconjug. Chem. 13 (4), 840–844.

Zwick, M.B., Shen, J.Q., Scott, J., 1998. Phage-displayed peptide libraries. Curr. Opin. Biotechnol. 9 (4), 427–436.

Please cite this article in press as: Larbanoix, L., et al., Potential amyloid plaque-specific peptides for the diagnosis of Alzheimer's disease. Neurobiol. Aging (2008), doi:10.1016/j.neurobiolaging.2008.09.021